Core-hole jumping between heavy atoms enabled by retardation

Jaroslav Hofierka and Lorenz S. Cederbaum
Theoretische Chemie, Physikalisch-Chemisches Institut, Universität Heidelberg, Im Neuenheimer Feld 229, D-69120 Heidelberg, Germany

(Received 6 March 2024; accepted 18 April 2024; published 9 May 2024)

In interatomic Coulombic decay (ICD) an excited neutral atom or excited ion transfers its excess energy to ionize a neighboring atom. If the excitation or ionization involves valence electrons, the process is efficient (typically in the femtosecond regime), becomes more efficient the more neighbors are present, and often dominates all other relaxation processes. The situation changes when considering the excitation or ionization of core electrons. For light atoms, core-level ICD is inferior to Auger decay, but still a relevant relaxation pathway. For heavy atoms the excess energy is enormous and by consulting the usual asymptotic equation for the ICD rate one can only conclude the deep core-level ICD to be negligible. Retardation effects due to the finite speed of light strongly change the asymptotic behavior of the ICD rate, in particular for deep core levels. The impact of retardation is investigated in detail for deep core-level ICD. Several examples of heavy atoms undergoing ICD with heavy neighbors are explicitly studied and general conclusions are drawn.

DOI: 10.1103/PhysRevA.109.052812

I. INTRODUCTION

A vacancy in a deep core electron level of an atom, created by means of hard x-ray radiation, is usually filled very rapidly by an electron from a higher level, releasing excess energy using one of multiple possible pathways. For lighter atoms, or shallow core levels of heavy atoms, the dominating pathway is the Auger process [1], where the so-called Auger electron is emitted. However, an x-ray photon can be emitted instead of the Auger electron. For first-row atoms, the x-ray emission rate is much smaller than the Auger decay rate, typically 10^3–10^6 times [1], yet it still has important implications in the field of x-ray emission spectroscopy (XES), see, e.g., Ref. [2]. In case of deepest levels of heavy atoms, the situation is reversed: the radiative decay dominates over the Auger process by several orders of magnitude [1]. In reality, atoms usually have neighbors and one can wonder whether nonlocal energy transfer is possible even for the deepest levels of heavy atoms.

Interatomic energy transfer processes between two or more atomic species are ubiquitous in nature and very widely studied both theoretically and experimentally. Interatomic Coulombic decay (ICD), originally predicted in 1997, see Refs. [3–5], is a highly efficient electronic energy transfer mechanism in weakly bound atomic (and molecular) systems. After an ionization of an atom, the initial vacancy of the ion is filled by a higher-lying electron and the emerging excess energy is transferred radiationlessly to a neighboring atom resulting in its ionization. If the excess energy from a single donor is insufficient to ionize the neighbor, a collective energy transfer from multiple donors to a single acceptor might be relevant, a process called collective ICD [6,7]. In the asymptotic limit of nonoverlapping electron clouds, the rate of ICD has been shown to decrease rapidly with both higher transferred energy E as $1/E^4$, and larger distance R between the participating species as $1/R^6$ [4]. In case of the core levels, however, the transferred energies are usually too large for the ICD rate to compete with the local (Auger and fluorescence) processes due to the aforementioned asymptotic behavior. On the other hand, the efficiency of ICD can be increased by increasing the number of nearest neighbors, as was recently shown experimentally in core-level ionized Kr clusters [8]. In this study, the relative efficiency of the ICD process with respect to the Auger decay (branching ratio) for the Kr clusters was reported to be about 2%. Core-level ICD was also observed following core ionization of metal cations in KCl and $CaCl_2$ solutions, with ICD-to-Auger branching ratios for K^+ and Ca^{2+} equal to 1.9% and 9.5% [9,10]. Finally, recent *ab initio* calculations indicated that for shallow core vacancies in rare-gas clusters, the ICD-to-Auger ratio is about 3% [11].

Recently, a novel theoretical description of ICD based on macroscopic quantum electrodynamics [12] indicated that the spatial (and energetic) range of ICD may be much larger than previously expected thanks to the finite speed of light. This relativistic retardation of the virtual photon coupling was also studied earlier in the context of the intermolecular phenomenon named Foerster resonance energy transfer (FRET) [13–15]. Crucially, with the retardation the asymptotic ICD rate includes a term independent of the virtual photon energy E, and decreases only with the square of the distance R between the participating species. In this work we revisit the earlier results on retarded ICD and calculate ICD rates and lifetimes for various pairs of heavy atoms, showing that the relativistic retardation enables the core-hole jumping to proceed in the picosecond regime even in the case of deepest core holes involving photon energies up to 100 keV.

II. THEORY

First, we review the underlying theory by following the line of discussion of mostly [12] and partly also [14]. Consider two atoms separated by a distance R large enough so that their mutual interaction is relatively weak. Then, the electronic structure of the composite system may be approximately considered as that of two individual species interacting through

the electromagnetic radiation field. The first, donor atom D decays from an initially core-ionized (excited) state to a lower excited state, releasing energy as a virtual photon, which is then absorbed by the second, acceptor atom A that undergoes ionization. The initial and final states of this ICD process will be denoted as $|i\rangle = |D^*\rangle|A\rangle|0\rangle$ and $|f\rangle = |D\rangle|A^+\rangle|0\rangle$, with the electromagnetic vacuum field denoted by $|0\rangle$. The final ion state $|A^+\rangle$ is assumed to include the emitted ICD electron. The rate Γ of this process can be determined as

$$\Gamma = 2\pi \sum_f |M_{fi}|^2 \delta(E_f - E_i), \tag{1}$$

where M_{fi} is a transition matrix element and $\delta(E_f - E_i)$ ensures the energy conservation between the initial and final states. The transition matrix element for an exchange of a single virtual photon can be computed as [12]

$$M_{fi} = \sum_{m=m_1,m_2} \frac{\langle f|H_{\rm int}|m\rangle\langle m|H_{\rm int}|i\rangle}{E_i - E_m}, \tag{2}$$

where the intermediate states m are two possible time orderings of the virtual photon exchange process: $|m_1\rangle = |D\rangle|A\rangle|1(\boldsymbol{r},\omega)\rangle$ and $|m_2\rangle = |D^*\rangle|A^+\rangle|1(\boldsymbol{r},\omega)\rangle$, where the photon is specified by its position $\boldsymbol{r}$ and frequency ω. The interaction Hamiltonian in the electric dipole approximation reads

$$\hat{H}_{\rm int} = -\hat{\boldsymbol{d}}_D \cdot \hat{\boldsymbol{E}}(\boldsymbol{r}_D) - \hat{\boldsymbol{d}}_A \cdot \hat{\boldsymbol{E}}(\boldsymbol{r}_A), \tag{3}$$

where $\hat{\boldsymbol{d}}$ is the dipole operator of the respective atom located at $\boldsymbol{r}_D$ or $\boldsymbol{r}_A$, and the radiation field $\hat{\boldsymbol{E}}$ can be expressed as a sum over modes

$$\hat{\boldsymbol{E}}(\boldsymbol{r}) = \mathcal{N} \sum_{\boldsymbol{k},\lambda} \sqrt{\hbar\omega_k}[\boldsymbol{\epsilon}_\lambda(\boldsymbol{k}) a_\lambda(\boldsymbol{k}) e^{i\boldsymbol{k}\cdot\boldsymbol{r}} - \bar{\boldsymbol{\epsilon}}_\lambda(\boldsymbol{k}) a_\lambda^\dagger(\boldsymbol{k}) e^{-i\boldsymbol{k}\cdot\boldsymbol{r}}], \tag{4}$$

with summations over wave vectors $\boldsymbol{k}$ and the polarization unit vectors $\boldsymbol{\epsilon}_\lambda(\boldsymbol{k})$. Note that the magnetic and multipole effects are formally neglected in the present treatment as they are expected to be small [16]. Substituting the interaction Hamiltonian [Eq. (3)] and the radiation field expansion [Eq. (4)] into Eq. (2) results in lengthy expressions that can be manipulated by performing the sum over polarization directions λ and wave vectors $\boldsymbol{k}$ (after converting the sum to an integral), leading to the expression [13–15]

$$\begin{aligned} M_{fi}(\omega, R) = \frac{e^{i\omega R/c}}{R^3}[&(\boldsymbol{d}_D \cdot \boldsymbol{d}_A - 3 \\ &\times (\boldsymbol{u}_R \cdot \boldsymbol{d}_D)(\boldsymbol{u}_R \cdot \boldsymbol{d}_A))(1 - i\omega R/c) \\ &- (\boldsymbol{d}_D \cdot \boldsymbol{d}_A - (\boldsymbol{u}_R \cdot \boldsymbol{d}_D)(\boldsymbol{u}_R \cdot \boldsymbol{d}_A))\omega^2 R^2/c^2], \end{aligned} \tag{5}$$

where $\boldsymbol{d}_D = \langle D^*|\hat{\boldsymbol{d}}_D|D\rangle$ and $\boldsymbol{d}_A = \langle A|\hat{\boldsymbol{d}}_A|A^+\rangle$ are the transition dipole moment integrals, $\boldsymbol{u}_R$ is the unit vector in the direction of $\boldsymbol{R} = \boldsymbol{r}_D - \boldsymbol{r}_A$, and R the magnitude of $\boldsymbol{R}$.

Assuming the situation $\omega R \ll c$, which corresponds to low photon energies and relatively short distances R, the well-known classical dipole-dipole interaction formula is obtained [17]:

$$M_{fi}(R) = \frac{1}{R^3}[\boldsymbol{d}_D \cdot \boldsymbol{d}_A - 3(\boldsymbol{u}_R \cdot \boldsymbol{d}_D)(\boldsymbol{u}_R \cdot \boldsymbol{d}_A)]. \tag{6}$$

In particular, if both dipoles are aligned parallel to $\boldsymbol{u}_R$, the interaction energy is twice that of the dipoles parallel to each other but perpendicular to $\boldsymbol{u}_R$ and this ratio is independent of the separation. In the retarded limit, given by $\omega R \gg c$, the leading term becomes [18]

$$M_{fi}(\omega, R) = \frac{\omega^2 e^{i\omega R/c}}{Rc^2}[\boldsymbol{d}_D \cdot \boldsymbol{d}_A - (\boldsymbol{u}_R \cdot \boldsymbol{d}_D)(\boldsymbol{u}_R \cdot \boldsymbol{d}_A)]. \tag{7}$$

Obviously in this case the matrix element is zero if both dipoles are aligned parallel to $\boldsymbol{u}_R$. Performing rotational averaging over the initial states, and summing over all possible final states [19,20], we obtain from Eq. (5) the following expression for the squared absolute value of the isotropic transition amplitude [13]:

$$|M_{fi}(\omega, R)|^2 = \frac{2}{9}|\boldsymbol{d}_D|^2|\boldsymbol{d}_A|^2 \left\{ \frac{3}{R^6} + \left(\frac{\omega}{c}\right)^2 \frac{1}{R^4} + \left(\frac{\omega}{c}\right)^4 \frac{1}{R^2} \right\}. \tag{8}$$

For the donor atom, the transition dipole is related to the emission of a photon with energy equal to the difference between the states involved in this transition. Thus we can introduce the spontaneous radiative decay rate (Einstein coefficient) $\gamma^{\rm rad}$ as [21]

$$|\boldsymbol{d}_D|^2 = \frac{3\hbar c^3}{4\omega^3}\gamma^{\rm rad}. \tag{9}$$

Further, the transition dipole matrix element $\boldsymbol{d}_A$ can be expressed via the direct photoionization cross section $\sigma_\omega^{\rm PI}$ of the acceptor atom [19]

$$|\boldsymbol{d}_A|^2 = \frac{3c}{4\pi^2\omega}\sigma_\omega^{\rm PI}. \tag{10}$$

Altogether this leads to the ICD rate[1]

$$\Gamma^{\rm ICD}(\omega, R) = \frac{1}{4\pi}\gamma^{\rm rad}\sigma_\omega^{\rm PI} \left\{ \left(\frac{c}{\omega}\right)^4 \frac{3}{R^6} + \left(\frac{c}{\omega}\right)^2 \frac{1}{R^4} + \frac{1}{R^2} \right\}, \tag{11}$$

where the first term is the standard (nonretarded) rate [4] and the other two terms are due to the retardation [12]. The last term in Eq. (11) is expected to dominate once $R > c/\omega$ is satisfied. For transition energies of 10 keV, this inequality holds whenever $R > 0.2$ Å. For comparison, note that the van der Waals radius of uranium is about 2.7 Å [22]. Thus for the deep core transitions of heavy atoms with energies above 10 keV, the final retarded term is expected to dominate the other terms by many orders of magnitude. For 100 keV and $R = 10$ Å, the enhancement factor is $(\omega R/c)^4/3 \approx 2 \times 10^{10}$.

Thus, while the standard ICD rate is quenched by high transition energies $\hbar\omega$, the retarded term is independent of this energy, although an implicit dependence is hidden in the radiative rate $\gamma^{\rm rad}$ and the photoionization cross section $\sigma_\omega^{\rm PI}$, as discussed below. It is worth noting that when considering higher-order effects (electric quadrupole, etc.) the final term maintains the $1/R^2$ dependence [15], while the asymptotics of the standard nonretarded term changes to $1/R^8$, $1/R^{10}$, and so on [4]. Also note that the presented formulas are asymptotic.

[1]Note that the expression in Ref. [12] is missing a factor of $1/\pi$ compared to the present treatment.

At short to intermediate distances, the orbital overlap of the respective atomic electron densities plays a significant role and can enhance the ICD rate by several orders of magnitude [4]. However, as the valence electrons are not directly involved in the ICD where the core electrons of both the donor and acceptor constitute the by far dominating channels, this overlap is expected to play a lesser role here. Nevertheless, one may expect the overlap of valence orbitals to enhance the ICD rate. However, the degree of orbital overlap depends on the specific choice of donor and acceptor species and is difficult to estimate, thus we neglect it completely in the present treatment.

Finally, the retarded term of Eq. (11) is repeated here again in practical units as retarded ICD decay width

$$\Gamma^{\rm ret}[\text{eV}] = \frac{1}{4\pi}\frac{\hbar\gamma^{\rm rad}[\text{eV}]\sigma_\omega^{\rm PI}[\text{kb}]}{(R[\text{Å}])^2}\times 10^{-5}, \qquad (12)$$

where the factor 10^{-5} comes from the conversion 1 kb = 10^{-5} Å^2. The corresponding lifetime is in general given by

$$\tau[s] = \frac{6.58\times 10^{-16}}{\Gamma[\text{eV}]}. \qquad (13)$$

III. RESULTS AND DISCUSSION

Let us now discuss specific examples of heavy atoms undergoing core-level ICD and present approximate decay widths and lifetimes. First, note that the radiative rates $\gamma^{\rm rad}$ of the deepest core ($1s$) holes increase steadily with atomic number Z even for very heavy atoms, with the corresponding lifetimes $\tau^{\rm rad} = 1/\gamma^{\rm rad}$ equal to a few attoseconds for elements as heavy as uranium [1]. These extremely fast transitions provide an essential ingredient for the efficiency of the core-level ICD process. The energies of the dominant $2p_{3/2} \to 1s$ transitions range from about 13 keV in Kr up to about 100 keV in U. Throughout this work, the radiative rates $\gamma^{\rm rad}$ for the individual transitions are obtained from earlier relativistic calculations performed by Scofield [23,24]. In these calculations, the electrons were treated relativistically and the effect of retardation was included.

While it is clear that the donor atom should preferably be as heavy as possible in order to maximize the core-level ICD rate, the choice of the acceptor atom is a bit less clear cut. One might be tempted to ionize a lighter element, e.g., a first-row atom such as O or F. Considering a transferred energy of 10 keV, for example, the photoionization cross sections $\sigma_\omega^{\rm PI}$ for these two atoms are about 150 barns (O) and 240 barns (F) [25], and decrease steeply with increasing energy. That is about two orders of magnitude lower than cross sections typical of heavier elements, even at much higher energies, as

TABLE I. Examples of deep core-level ICD in heavy atoms. Here, the initial core-hole decay on the donor atom is specified by the x-ray transition energy $\hbar\omega$ and the radiative decay width $\hbar\gamma^{\rm rad}$ taken from [23,24]. For the acceptor atom the total photoionization cross sections $\sigma_\omega^{\rm PI}$ evaluated at the respective transition energy are taken from tabulated results [25,26], with the core shell indicated in parentheses accounting for about 75% of the total $\sigma_\omega^{\rm PI}$ on average. The ICD rate $\Gamma^{\rm ICD}$ and lifetime $\tau^{\rm ICD}$ (see main text) are evaluated at $R = \sqrt{10}$ Å. The last column shows the enhancement factor due to retardation $k^{\rm ret} = (\omega R/c)^4/3$ for $R = \sqrt{10}$ Å.

Donor			Acceptor	Results at $R = \sqrt{10}$ Å		
X-ray Transition	$\hbar\omega$ (keV)	$\hbar\gamma^{\rm rad}$ (eV)	$\sigma_\omega^{\rm PI}$ (kb)	$\Gamma^{\rm ICD}$ (μeV)	$\tau^{\rm ICD}$ (ps)	$k^{\rm ret}$
U $2p_{3/2} \to 1s$	98.43	44.2	2.42[Rn($1s$)]	8.5	77	2.1×10^8
U $2p_{1/2} \to 1s$	94.65	27.6	2.29[Po($1s$)]	5.0	132	1.8×10^8
U $3p_{3/2} \to 1s$	111.3	10.2	1.94[Th($1s$)]	1.6	411	3.4×10^8
Pa $2p_{3/2} \to 1s$	95.86	42.1	2.50[At($1s$)]	8.4	78	1.9×10^8
Th $2p_{3/2} \to 1s$	93.35	40.7	2.59[Po($1s$)]	8.4	78	1.7×10^8
Ac $2p_{3/2} \to 1s$	90.88	38.7	2.69[Bi($1s$)]	8.3	79	1.5×10^8
Te $2p_{3/2} \to 1s$	27.47	4.50	9.94[Pb($2s$)]	3.6	183	1.3×10^6
Cd $2p_{3/2} \to 1s$	23.17	3.23	34.3[Pu($2s$)]	8.8	75	6.3×10^5
Ag $2p_{3/2} \to 1s$	22.16	2.96	36.4[U($2s$)]	8.8	75	5.3×10^5
Pd $2p_{3/2} \to 1s$	21.18	2.71	38.3[Pa($2s$)]	8.3	79	4.4×10^5
Ru $2p_{3/2} \to 1s$	19.28	2.25	42.4[Ra($2s$)]	7.6	87	3.0×10^5
Zr $2p_{3/2} \to 1s$	15.77	1.50	48.1[Bi($2p$)]	5.7	115	1.4×10^5
Rb $2p_{3/2} \to 1s$	13.40	1.08	61.1[Pt($2p$)]	5.3	124	7.1×10^4
Kr $2p_{3/2} \to 1s$	12.65	0.96	73.7[Re($2s$)]	5.6	117	5.6×10^4

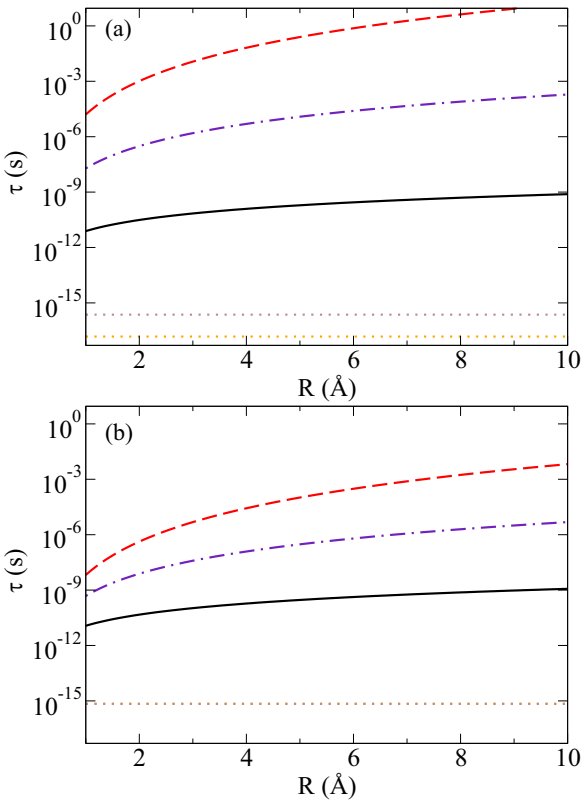

FIG. 1. The distance dependence of the nonretarded (dashed), intermediate (dot-dashed), and retarded (solid) contributions to the ICD lifetime $\tau^{\rm ICD}$ for the core-level ICD between (a) U and Rn and (b) Kr and Re. Note that these results are based on asymptotic formulas, which assume that the participating orbitals on individual atoms do not overlap. We expect that orbital overlap will lower the ICD lifetimes at short distances and that the presence of more neighbors can significantly shorten the ICD lifetimes (see text). The Auger and radiative lifetimes of the initial holes are also shown for comparison as brown and orange dotted lines for U in (a) and Kr in (b). For Kr the Auger and radiative lifetimes are very similar.

shown in Table I. Thus the ICD rate is expected to be higher by about two orders of magnitude when a heavy atom is chosen as the acceptor instead of a light atom. Here we use total photoionization cross sections $\sigma_\omega^{\rm PI}$ from tabulated results of relativistic calculations presented in Refs. [25,26], evaluated at energies that are as close as possible to the transition energies in question. Small discrepancies (<10%) between the two sources of data are of little importance for the present study. Also note that the partial photoionization cross section of the deepest ionizable shell contributes about 75% of the total cross section [26].

Thus, by taking a heavy acceptor atom as the ICD partner of the heavy donor atom, the product $\gamma^{\rm rad} \times \sigma_\omega^{\rm PI}$ can be maximized. In Table I, the donor transition energies are matched with the ionization thresholds of core-level subshells of the acceptor atoms, such that the transferred energy is just above the core-shell ionization threshold. Note that as the transition energy $\hbar\omega$ decreases, so does the radiative rate $\gamma^{\rm rad}$, while the photoionization cross section $\sigma_\omega^{\rm PI}$ increases at the same time, meaning that the product $\gamma^{\rm rad} \times \sigma_\omega^{\rm PI}$ remains approximately constant. Thus, for example, the ICD rate (lifetime) is about the same for the pair of U and the slightly lighter Rn on the one hand, and Ag and the heavier U on the other, assuming the same interatomic distance $R = \sqrt{10}$ Å throughout Table I for simplicity. This choice of R corresponds to the distance of Pb and Te atoms in the PbTe solid [27] (see below). For the pairs U-Rn, and Kr-Re, the dependence of the core-hole ICD lifetime on the atomic distance is shown in Fig. 1 independently for each of the terms in Eq. (11). The retardation enhancement for U-Rn is about 6–10 orders of magnitude in the spatial range of 1–10 Å while for the pair Kr-Re the corresponding enhancement amounts to 4–7 orders of magnitude. For comparison, the Auger lifetimes of the 1s holes are 0.7 fs for Kr and 0.2 fs for U (the corresponding decay widths are 0.9 eV for Kr and 2.9 eV for U [28]) and thus are lower than ICD lifetimes by about five orders of magnitude.

In real-life systems, such as solids, atoms have many neighbors allowing the core-level ICD to become relevant and experimentally accessible. Let us for illustrative purposes consider an example of Pb and Te atoms arranged in a simple cubic (rock salt) structure of the PbTe solid [27]. Taking into account the first coordination shell with six neighbors, the overall ICD rate following the $2p_{3/2} \rightarrow 1s$ transition in Te is expected to be six times larger than the single-pair ICD rate shown in Table I (see, e.g., Refs. [8,29] for a discussion of the pair approximation where the total ICD rate is given as the sum of the single-pair rates). Due to the retardation, the overall ICD rate $\Gamma^{\rm ICD}$ grows quickly when we take into account the neighboring Pb atoms. In particular, in addition to the nearest six Pb atoms at distance $R = \sqrt{10}$ Å there are eight Pb atoms at distance $R = \sqrt{30}$ Å, 24 Pb atoms at $R = \sqrt{50}$ Å, 30 Pb atoms at $R = \sqrt{90}$ Å, and 24 Pb atoms at $R = \sqrt{110}$ Å, altogether leading to the enhancement of the ICD rate by a factor of 19. Increasing further the number of neighbors can increase substantially the total ICD rate, which raises the need for investigating the range of validity of the pair approximation for deep core electrons of heavy atoms. This investigation is beyond the scope of this paper and is left for the future.

IV. BRIEF CONCLUSION

In conclusion, there is a non-negligible probability of a deep core-hole jumping from one heavy atom to another due to the relativistic retardation. For the pairs of heavy atoms considered in this work, the calculated ICD lifetimes are of the order of tens to hundreds of picoseconds. The present asymptotic ICD rate expression is expected to provide a lower bound to the correct ICD rate. Due to the retardation, which allows for the participation of many more neighbors, the ICD rate can be enhanced significantly. By discussing an example of the PbTe solid, we suggest that the deep core-level ICD process can be experimentally observable. In particular, the core-level ICD process produces electrons, which can be unambiguously identified and clearly distinguished from Auger electrons. Finally, the described mechanism could be extended to the case where one or both of the donor-acceptor pair is a molecule. In such a case the photoionization cross section might be increased such that the ICD efficiency becomes higher.

ACKNOWLEDGMENT

Financial support by the Deutsche Forschungsgemeinschaft (DFG) (Grant No. CE 10/56-1) is gratefully acknowledged.

[1] M. O. Krause, Atomic radiative and radiationless yields for K and L shells, J. Phys. Chem. Ref. Data **8**, 307 (1979).

[2] J. A. Van Bokhoven and C. Lamberti, *X-Ray Absorption and X-Ray Emission Spectroscopy: Theory and Applications* (John Wiley & Sons, New York, 2016), Vol. 1.

[3] L. S. Cederbaum, J. Zobeley, and F. Tarantelli, Giant intermolecular decay and fragmentation of clusters, Phys. Rev. Lett. **79**, 4778 (1997).

[4] V. Averbukh, I. B. Müller, and L. S. Cederbaum, Mechanism of interatomic coulombic decay in clusters, Phys. Rev. Lett. **93**, 263002 (2004).

[5] T. Jahnke, U. Hergenhahn, B. Winter, R. Dörner, U. Frühling, P. V. Demekhin, K. Gokhberg, L. S. Cederbaum, A. Ehresmann, A. Knie, and A. Dreuw, Interatomic and intermolecular coulombic decay, Chem. Rev. **120**, 11295 (2020).

[6] V. Averbukh and P. Kolorenč, Collective interatomic decay of multiple vacancies in clusters, Phys. Rev. Lett. **103**, 183001 (2009).

[7] L. S. Cederbaum and A. I. Kuleff, An ensemble of excited molecules collectively emits multiple-frequency real and virtual photons, J. Chem. Phys. **160**, 064306 (2024).

[8] C. Küstner-Wetekam, L. Marder, D. Bloß, C. Honisch, N. Kiefer, C. Richter, S. Rubik, R. Schaf, C. Zindel, M. Förstel, K. Gokhberg, A. Knie, U. Hergenhahn, A. Ehresmann, P. Kolorenč, and A. Hans, Experimental quan-

tification of site-specific efficiency of interatomic coulombic decay after inner shell ionization, Commun. Phys. **6**, 50 (2023).

[9] W. Pokapanich, H. Bergersen, I. L. Bradeanu, R. R. T. Marinho, A. Lindblad, S. Legendre, A. Rosso, S. Svensson, M. Tchaplyguine, N. V. Kryzhevoi, and L. S. Cederbaum, Auger electron spectroscopy as a probe of the solution of aqueous ions, J. Am. Chem. Soc. **131**, 7264 (2009).

[10] W. Pokapanich, N. V. Kryzhevoi, N. Ottosson, S. Svensson, L. S. Cederbaum, G. Öhrwall, and O. Björneholm, Ionic-charge dependence of the intermolecular coulombic decay time scale for aqueous ions probed by the core-hole clock, J. Am. Chem. Soc. **133**, 13430 (2011).

[11] L. Liu, P. Kolorenč, and K. Gokhberg, Efficiency of core-level interatomic Coulombic decay in rare-gas dimers, Phys. Rev. A **101**, 033402 (2020).

[12] J. L. Hemmerich, R. Bennett, and S. Y. Buhmann, The influence of retardation and dielectric environments on interatomic Coulombic decay, Nature Commun. **9**, 2934 (2018).

[13] G. A. Jones and D. S. Bradshaw, Resonance energy transfer: From fundamental theory to recent applications, Front. Phys. **7**, 100 (2019).

[14] G. J. Daniels, R. D. Jenkins, D. S. Bradshaw, and D. L. Andrews, Resonance energy transfer: The unified theory revisited, J. Chem. Phys. **119**, 2264 (2003).

[15] A. Salam, A general formula for the rate of resonant transfer of energy between two electric multipole moments of arbitrary order using molecular quantum electrodynamics, J. Chem. Phys. **122**, 044112 (2005).

[16] J. H. Scofield, Radiative decay rates of vacancies in the K and L shells, Phys. Rev. **179**, 9 (1969).

[17] J. A. D. Matthew and Y. Komninos, Transition rates for interatomic Auger processes, Surf. Sci. **53**, 716 (1975).

[18] A. B. Voitkiv and B. Najjari, Two-center dielectronic recombination and resonant photoionization, Phys. Rev. A **82**, 052708 (2010).

[19] I. I. Sobelman, G. K. Woodgate, and D. T. Haar, *Introduction to the Theory of Atomic Spectra, International Series of Monographs in Natural Philosophy* (Elsevier Science, Amsterdam, 2016).

[20] J. Fedyk, K. Gokhberg, and L. S. Cederbaum, Theory of double ionization of a neighboring molecule by interatomic Coulombic decay, Phys. Rev. A **103**, 022816 (2021).

[21] A. P. Thorne, *Spectrophysics* (Springer, Netherlands, 2012).

[22] J. Echeverría and S. Alvarez, The borderless world of chemical bonding across the van der Waals crust and the valence region, Chem. Sci. **14**, 11647 (2023).

[23] J. H. Scofield, Exchange corrections of K X-ray emission rates, Phys. Rev. A **9**, 1041 (1974).

[24] J. H. Scofield, Relativistic hartree-slater values for K and L X-ray emission rates, At. Data Nucl. Data Tables **14**, 121 (1974).

[25] W. J. Veigele, Photon cross sections from 0.1 keV to 1 MeV for elements $Z = 1$ to $Z = 94$, At. Data Nucl. Data Tables **5**, 51 (1973).

[26] J. H. Scofield, Theoretical photoionization cross sections from 1 to 1500 keV, Technical Report No. UCRL–51326, California University, Livermore, Lawrence Livermore Laboratory (1973).

[27] P. Bauer Pereira, I. Sergueev, S. Gorsse, J. Dadda, E. Müller, and R. P. Hermann, Lattice dynamics and structure of GeTe, SnTe and PbTe, Physica Status Solidi B **250**, 1300 (2013).

[28] M. H. Chen, B. Crasemann, and H. Mark, Relativistic K -shell Auger rates, level widths, and fluorescence yields, Phys. Rev. A **21**, 436 (1980).

[29] N. V. Kryzhevoi, V. Averbukh, and L. S. Cederbaum, High activity of helium droplets following ionization of systems inside those droplets, Phys. Rev. B **76**, 094513 (2007).